Mechanism for the Pseudoelastic Behavior of FCC Shape Memory Nanowires

X. Guo · W. Liang · M. Zhou

Abstract Pseudoelasticity and shape memory have been recently discovered in single-crystalline FCC nanowires of Cu, Ni, Au and Ag. The deformation mechanism responsible for this novel behavior is surface-stress-driven reorientations of the FCC lattice structure. A mechanism-based continuum model has been developed for the lattice reorientation process during loading through the propagation of a single twin boundary. Here, this model is extended to the nucleation, propagation and annihilation of multiple twin boundaries associated with the reverse reorientation process during unloading. The extended model captures the major characteristics of the loading and unloading behavior and highlights the dominating effect of the evolution of twin boundary structure on the pseudoelasticity.

Keywords Pseudoelasticity · Nanowire ·
Micromechanical continuum model · Reorientation ·
Twin boundary

Introduction

Recent research has revealed a novel shape memory effect and pseudoelastic behavior in single-crystalline face-centered cubic (FCC) nanowires of Cu, Ni, Au and Ag [1–6]. This behavior is associated with a reversible lattice reorientation process within the FCC crystalline structure and is driven by the surface stress and high surface-to-volume ratios of the nanowires. The existence of this

X. Guo · W. Liang · M. Zhou (✉)
The George W. Woodruff School of Mechanical Engineering,
Georgia Institute of Technology,
Atlanta, GA 30332-0405, USA
e-mail: min.zhou@gatech.edu

behavior or the lack of it depends on the twinnability of the material, wire size and temperature [2, 7]. A micro-mechanical continuum model has been developed to characterize the loading process of this unique tensile behavior [8, 9]. This model focuses on the lattice reorientation that occurs through the propagation of a single twin boundary. Although the initial $\langle 110 \rangle / \{111\}$ configuration [Fig. 1(a)] and the deformed $\langle 001 \rangle / \{100\}$ configuration [Fig. 1(b)] of the nanowire have the same FCC structure, the former has a lower free energy level than the latter primarily because $\{111\}$ surfaces have lower energies than $\{100\}$ surfaces and surface energies dominate the total energy. Since different crystalline directions exhibit different physical responses, the lattice reorientation process can be phenomenologically considered as a phase transformation which is necessary for pseudoelastic and shape memory behaviors. In the treatment in [8, 9], this process is decomposed into a non-dissipative part and a dissipative part, in accordance with the first law of thermodynamics. The non-dissipative part describes the smooth equilibrium transition between the $\langle 110 \rangle / \{111\}$ and $\langle 001 \rangle / \{100\}$ configurations and was studied via constrained strain energy minimization. The dissipative part relates to the process of twin boundary propagation which involves overcoming the energy barriers between phase-equilibrium states.

In this paper, we extend the analysis to the reverse lattice reorientation during unloading. The dissipation arises from the propagation which also occurs during loading and the nucleation and annihilation of multiple twin boundaries which occur only during unloading. The twin boundaries have the same crystalline orientation, surface area and structure and, therefore, are assumed to possess the same amount of interfacial energy. They are also assumed to have the same energy dissipation rate as they propagate. The
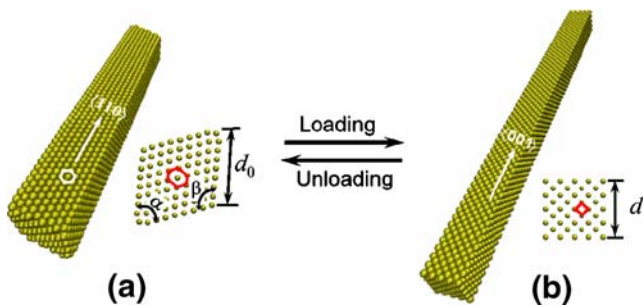
Fig. 1 Configurations of FCC metal nanowires: (**a**) a self-equilibrated <110>/{111} wire with rhombic cross-section (α=70.5° and β=109.5°) and (**b**) a stretched <001>/{100} wire with square cross-section [8]

model prediction is in good agreement with the results of molecular dynamics (MD) simulations for wire sizes between 1.5 and 2.5 nm and for temperatures between 150 and 450 K.

Tensile Loading and Unloading Behavior of Cu Nanowires

During isothermal, quasi-static tensile deformation, Cu wires with the $\langle 110 \rangle/\{111\}$ configuration [Fig. 1(a)] and lateral dimensions under approximately 5 nm exhibit a stress–strain behavior drastically different from that of the corresponding bulk Cu, as shown in Fig. 2. Specifically, the stress–strain curve consists of four elastic deformation stages (O→A, C→D, C→E, and F→O) and two intervening stages of inelastic deformation over wide ranges of strain (B→C and E→F). This behavior arises from a unique underlying deformation process:

1. Between O and A, the $\langle 110 \rangle/\{111\}$-structured wire undergoes elastic stretching;
2. Between B and C, a gradual transform from the $\langle 110 \rangle/\{111\}$ configuration to the $\langle 001 \rangle/\{100\}$ configuration [Fig. 1(b)] occurs through lattice reorientation via the propagation of a single twin boundary;
3. Between C and D, the $\langle 001 \rangle/\{100\}$-structured wire undergoes elastic stretching;
4. Between C and E, the $\langle 001 \rangle/\{100\}$-structured wire (if unloading is carried out after the completion of transformation under loading) or the wire with a $\langle 110 \rangle/\{111\}$ region and a $\langle 001 \rangle/\{100\}$ region (if unloading is carried out before the completion of transformation under loading) undergoes elastic recovery;
5. Between E and F, reverse transformation from the $\langle 001 \rangle/\{100\}$ configuration to the $\langle 110 \rangle/\{111\}$ configuration occurs through reverse lattice reorientation. This process involves the propagation, nucleation and annihilation of multiple twin boundaries which cause significant oscillations in the stress in the nanowire;

6. Between F and O, the $\langle 110 \rangle/\{111\}$-structured wire unloads elastically and returns to the original undeformed state, thus completing the pseudoelastic hysteresis loop.

Although not the focus of this paper, further extension beyond D results in the yielding, necking and fracture of the $\langle 001 \rangle/\{100\}$-structured wire [10]. The unique $\langle 110 \rangle/\{111\}$-to-$\langle 001 \rangle/\{100\}$ lattice reorientation and the reverse $\langle 001 \rangle/\{100\}$-to-$\langle 110 \rangle/\{111\}$ lattice reorientation processes [B→C and E→F in Fig. 2(a)] are the key to the pseudoelastic behavior. The forward lattice reorientation occurs through the propagation of a coherent twin boundary separating the initial $\langle 110 \rangle/\{111\}$ phase and the new $\langle 001 \rangle/\{100\}$ phase. The twin boundary propagates through successive nucleation, glide and annihilation of a partial dislocation. These events are the source of energy dissipation during loading [11]. As the twin boundary sweeps through the wire, the wire progressively transforms into the new $\langle 001 \rangle/\{100\}$ phase. Upon arrival of the twin boundary at the far end of the wire [corresponding to point C in Fig. 2(a)], the whole wire is in the $\langle 001 \rangle/\{100\}$ phase [2, 3]. During unloading, the $\langle 001 \rangle/\{100\}$-structured wire first deforms elastically and then spontaneously transforms
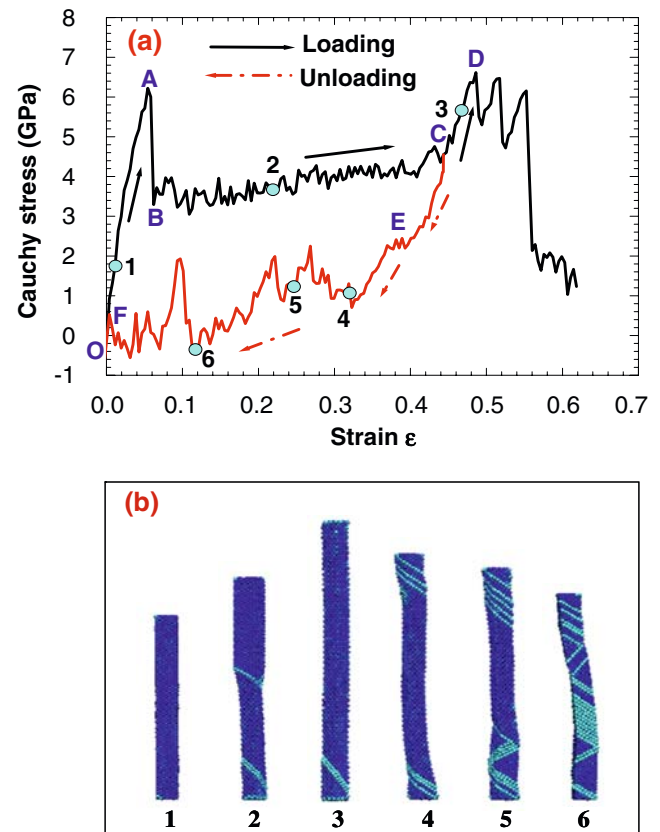
Fig. 2 A 1.8×1.8 nm Cu wire under quasi-static tensile loading and unloading at 200 K, (**a**) stress–strain curve, (**b**) configurations at different stages of deformation

back to the original $\langle 110\rangle/\{111\}$ configuration via the reverse lattice reorientation process. This spontaneous lattice reorientation occurs because the $\langle 110\rangle/\{111\}$ configuration has a lower total energy and is more stable than the $\langle 001\rangle/\{100\}$ configuration. Such a novel pseudoelastic behavior and associated shape memory effect are driven by high surface stresses due to the high surface-to-volume ratios of the nanowires. The extraordinarily large reversible strains (up to 50%) of the wires are primarily due to the large transformation strain (ε_{tr}=0.414) associated with the forward and reverse lattice reorientations [2, 3].

Thermodynamics of Loading and Unloading

The reversible lattice reorientation process can be decomposed into a thermodynamically reversible part and a thermodynamically irreversible part. For the reversible part, it is assumed that the wire smoothly goes through a series of phase-equilibrium states. However, the actual transitions between the equilibrium states are not smooth because there are barriers associated with the propagation of a twin boundary during loading and with the nucleation, propagation and annihilation of twin boundaries during unloading. The work required to overcome the barriers is released when the system settles into a metastable state. This release produces heat which is dissipated and constitutes the irreversible part of the deformation process.

The first law of thermodynamics relates the change in internal energy, work input and dissipation as

$$\mathrm{d}\,W = \mathrm{d}\,U + \mathrm{d}\,Q, \tag{1}$$

where $\mathrm{d}W$ is the work done by applied load, $\mathrm{d}U$ is the change in internal energy in the nanowire and $\mathrm{d}Q$ is the energy dissipated in the form of heat. During the elastic deformation [O→A, C→D, C→E and F→O in Fig. 2(a)], there is no dissipation (i.e., $\mathrm{d}Q$=0). Hence,

$$\mathrm{d}\,W = \mathrm{d}\,U. \tag{2}$$

However, when phase transformation occurs [B→C and E→F in Fig. 2(a)], $|\mathrm{d}Q|>0$.

Table 1 lists the signs of the three thermodynamic quantities during loading and unloading. In this convention, work done on the system and heat dissipated (flowing out of the system) are considered positive and vice versa.

Table 1 Signs convention for mechanical work, internal energy and dissipation during loading and unloading

	dW	dU	dQ
Loading ($\langle 110\rangle/\{111\} \rightarrow \langle 001\rangle/\{100\}$)	+	+	+
Unloading $\langle 001\rangle/\{100\} \rightarrow \langle 110\rangle/\{111\}$)	−	−	+

During loading, external work $\mathrm{d}W$ is positive and part of it goes toward increasing the strain energy $\mathrm{d}U$ and part of it is dissipated as heat $\mathrm{d}Q$. The relation can be written as

$$|\mathrm{d}\,W| = |\mathrm{d}\,U| + |\mathrm{d}\,Q|. \tag{3}$$

During unloading, the strain energy in the nanowire decreases. Part of the decrease is expended on providing work to the surrounding and part of it is dissipated as heat. The relation is

$$|\mathrm{d}\,W| = |\mathrm{d}\,U| - |\mathrm{d}\,Q|. \tag{4}$$

The total mechanical work done by applied load is

$$W = V_0 \int_0^\varepsilon \sigma\,\mathrm{d}\,\varepsilon, \tag{5}$$

where V_0 is the initial volume of the wire in the unstressed state, and σ and ε are the nominal stress and strain, respectively. The nominal strain ε is the overall average nominal strain with the self-equilibrated $\langle 110\rangle/\{111\}$ wire as the reference state. Specifically,

$$\varepsilon = \frac{\delta}{l_0}, \tag{6}$$

where δ is the total elongation and l_0 is the length of the initial unstressed $\langle 110\rangle/\{111\}$ wire. The nominal stress σ is given by

$$\sigma = \frac{1}{V_0}\frac{\partial W}{\partial \varepsilon}. \tag{7}$$

Thus, the stresses during loading and unloading are, respectively,

$$\sigma = \begin{cases} \frac{1}{V_0}\frac{\mathrm{d}U}{\mathrm{d}\varepsilon} + \frac{1}{V_0}\frac{\mathrm{d}Q}{\mathrm{d}\varepsilon} = \sigma_e + \sigma_{dissip}, & \text{during loading; and} \\ \frac{1}{V_0}\frac{\mathrm{d}U}{\mathrm{d}\varepsilon} - \frac{1}{V_0}\frac{\mathrm{d}Q}{\mathrm{d}\varepsilon} = \sigma_e - \sigma_{dissip}, & \text{during unloading.} \end{cases} \tag{8}$$

Here, σ_e is the part of the stress needed to drive the transition of the phase-equilibrium states and the elastic deformation of the phases. It is associated with strain energy. It so happens that during loading only equilibrium transition of states occurs and the elastic strains in the phases are constant. On the other hand, σ_{dissip} is the part of the stress associated with energy dissipation.

To analyze the transformation, a characterization of the behaviors of the $\langle 110\rangle/\{111\}$ and $\langle 001\rangle/\{100\}$ phases in the wires is needed. Similar to the overall strain ε, ε_{110} and ε_{001} denote the engineering strains of the $\langle 110\rangle/\{111\}$ and $\langle 001\rangle/\{100\}$ phases, respectively, with the reference states being the corresponding unstressed self-equilibrium states. Obviously, the stresses in the phases are

$$\left. \begin{array}{l} \sigma_{110} = \frac{\mathrm{d}u_{110}}{\mathrm{d}\varepsilon_{110}} \quad \text{and} \\ \sigma_{001} = \frac{\mathrm{d}u_{001}}{\mathrm{d}\varepsilon_{001}}, \end{array} \right\} \tag{9}$$

where u_{110} and u_{001} are strain energy density functions of the two phases, respectively. Let A_{110} denote the area of the rhombic cross-section of the $\langle 110 \rangle / \{111\}$ phase and A_{001} denote the area of the square cross-section of the $\langle 001 \rangle / \{100\}$ phase. Since the volume change associated with the transformation is extremely small, the average Cauchy stress in the wire can be calculated as

$$\tilde{\sigma} = \frac{\sigma A_{110}}{A} = \frac{\sigma A_{110} l}{Al} = \frac{\sigma A_{110} l}{A_{110} l_0} = \sigma(1 + \varepsilon), \tag{10}$$

where A is the average current cross-sectional area and l is current length of the wire.

Elastic Part of Behavior

Consider a phase-equilibrium state corresponding to a nominal strain ε in which two phases coexist and are separated by a single twin boundary. Each phase is elastically stretched. Therefore, the following field equations are satisfied:

$$\varepsilon_i = \frac{d\delta_i}{dx} \quad \text{in each phase} \tag{11}$$

and

$$\delta^+ = \delta^- \quad \text{at the twin boundary.} \tag{12}$$

Here, δ_i is the axial displacement of the wire. For the $\langle 110 \rangle / \{111\}$ phase, $i=110$ and $\delta=\delta_{110}$; for the $\langle 001 \rangle / \{100\}$ phase, $i=001$ and $\delta_i=\delta_{001}$. Similarly, ε_i is the local strain in the wire with $\varepsilon_i=\varepsilon_{110}$ in the $\langle 110 \rangle / \{111\}$ phase and $\varepsilon_i=\varepsilon_{001}$ in the $\langle 001 \rangle / \{100\}$ phase. δ^+ and δ^- denote the limiting values of the displacement on the two sides of the twin boundary. Equations (11) and (12) imply that the displacement is continuous within each phase and across the twin boundary.

The total strain ε includes contributions not only from the elastic strains in the two phases (ε_{110} and ε_{001}) but also from the strain (ε_{tr}) due to the phase transformation. Specifically,

$$\varepsilon = \frac{l - l_0}{l_0} \tag{13}$$

with

$$l = l_{110} + l_{001}. \tag{14}$$

Here, l_{110} and l_{001} are, respectively, the current lengths of the $\langle 110 \rangle / \{111\}$ and $\langle 001 \rangle / \{100\}$ phases corresponding to the total nominal strain ε. Note that

$$\left. \begin{array}{l} l_{110} = l_{110}^0 (1 + \varepsilon_{110}) \quad \text{and} \\ l_{001} = l_{001}^0 (1 + \varepsilon_{001}), \end{array} \right\} \tag{15}$$

where l_{110}^0 and l_{001}^0 are the lengths of the $\langle 110 \rangle / \{111\}$ and $\langle 001 \rangle / \{100\}$ phases in their unstressed states, respectively. Another kinematic constraint is that the sum of the equivalent stress-free lengths of the untransformed $\langle 110 \rangle / \{111\}$ phase and the transformed $\langle 110 \rangle / \{111\}$ phase must be equal to the length of the initial undeformed wire, i.e.,

$$l_{110}^0 + \frac{l_{001}^0}{1 + \varepsilon_{tr}} = l_0. \tag{16}$$

Here, $l_{001}^0 / (1 + \varepsilon_{tr})$ is the length of the transformed $\langle 110 \rangle / \{111\}$ phase as calculated from the length of the corresponding $\langle 001 \rangle / \{100\}$ phase. The above relation can be regarded as a statement of the conservation of mass.

In addition to the above kinematic relations, the stress field in each phase must satisfy the force balance condition. Specifically,

$$\frac{d\sigma_i}{dx} = 0 \quad \text{in each phase} \tag{17}$$

and

$$\sigma_{110} A_{110} = \sigma_{001} A_{001} \quad \text{at the phase boundary}. \tag{18}$$

Here, σ_i is the axial stress in the wire. For the $\langle 110 \rangle / \{111\}$ phase, $\sigma_i=\sigma_{110}$; for the $\langle 001 \rangle / \{100\}$ phase, $\sigma_i=\sigma_{001}$. Equations (17) and (18) imply that the force is continuous within each phase and across the twin boundary, and the stress is uniform within each phase.

A system in equilibrium has the minimum strain energy. Therefore, the phase equilibrium state of the wire can be obtained by minimizing the total strain energy subject to the force balance and kinematics constraints. The twin boundaries have the same crystalline orientation, surface area and structure, therefore, they are assumed to possess the same amount of interface energy (u_{int}). Thus, the total strain energy of the wire is composed of the strain energy of each phase and the interface energy, i.e.,

$$U = \int_{V_{110}} u_{110}(\varepsilon_{110}) \, dV + \int_{V_{001}} u_{001}(\varepsilon_{001}) \, dV + Nu_{int}, \tag{19}$$

where $V_{110} = A_{110} l_{110}^0$ and $V_{001} = A_{001} l_{001}^0$ are the initial unstressed volumes of the $\langle 110 \rangle / \{111\}$ and $\langle 001 \rangle / \{100\}$ phases, respectively, and N is the total number of mobile phase boundaries. During loading, $N=1$. During unloading, N changes whenever a nucleation or annihilation event occurs. Let $\varepsilon_1^c, \varepsilon_2^c, \cdots \varepsilon_n^c$ denote the values of the overall strain ε of the wire at which twin boundary nucleation or annihilation occurs. These events are associated with abrupt changes in the length fractions (l_{110}/l and l_{001}/l) of the two phases. Note that between any two successive events $\left[(\varepsilon_1^c > \varepsilon > \varepsilon_2^c), \right.$

$\left(\varepsilon_2^c > \varepsilon > \varepsilon_3^c\right), \cdots$ and $\left(\varepsilon_{n-1}^c > \varepsilon > \varepsilon_n^c\right)]$, N is constant. The overall variation of N is,

$$
N = \begin{cases} 0 & \text{elastic deformation } (O \rightarrow A, C \rightarrow D, \text{Fig.2a}); \\ 1 & \text{lattice reorientation during loading } (B \rightarrow C); \\ \text{constant} & \text{reverse lattice reorientation during unloading } \left(\varepsilon_{i-1}^c > \varepsilon > \varepsilon_i^c\right). \end{cases}
\tag{20}
$$

Prediction of the critical strains $\left(\varepsilon_i^c\right)$ requires a quantification of the energy barriers for the nucleation, annihilation and interactions of twin boundaries. This quantification is not available at this time without knowledge of the actual structural evolution paths or without a comprehensive characterization of the energy landscape accounting for all possible structural states. Here, these critical strain values are taken from the results of MD calculations and used to obtain the corresponding stresses in the wires through minimization of the total strain energy of the wire [equation (19)] for each and all stages of deformation during which the number of twin boundaries N is piecewise constant $\left[\left(\varepsilon_1^c > \varepsilon > \varepsilon_2^c\right), \left(\varepsilon_2^c > \varepsilon > \varepsilon_3^c\right), \cdots \text{ and } \left(\varepsilon_{n-1}^c > \varepsilon > \varepsilon_n^c\right)\right]$.

During the lattice reorientation in loading, the length fraction of each phase changes continuously and phase transformation is a smooth process. Details of the constrained energy minimization defined by equations (11)–(19) can be found in [8, 9]. The solution yields the elastic stresses (σ_{110} and σ_{001}), strains (ε_{110} and ε_{001}), and the length fractions (l_{110}/l and l_{001}/l) of the two phases at each level of ε. It is found that in each period of constant N, σ_{110} and σ_{001} are constant. For the transformation via the propagation of twin boundaries, equations (13)–(16) yield the lengths of the phases as

$$
\left.\begin{aligned}
l_{110} &= \frac{(1+\varepsilon_{110})(\varepsilon_{tr}+\varepsilon_{001}+\varepsilon_{tr}\varepsilon_{001}-\varepsilon)}{(\varepsilon_{tr}-\varepsilon_{110}+\varepsilon_{001}+\varepsilon_{tr}\varepsilon_{001})} l_0 \quad \text{and} \\
l_{001} &= \frac{(1+\varepsilon_{tr})(\varepsilon-\varepsilon_{110})(1+\varepsilon_{001})}{(\varepsilon_{tr}-\varepsilon_{110}+\varepsilon_{001}+\varepsilon_{tr}\varepsilon_{001})} l_0.
\end{aligned}\right\}
\tag{21}
$$

Consequently, the volumes of the phases are

$$
\left.\begin{aligned}
V_{001} &= (a + b\varepsilon)V_0 \quad \text{and} \\
V_{110} &= (c + d\varepsilon)V_0,
\end{aligned}\right\}
\tag{22}
$$

with the constants (note that the strains in the phases ε_{001} and ε_{110} remain constant) being

$$
\left.\begin{aligned}
a &= -\frac{(1+\varepsilon_{tr})(1+\varepsilon_{001})\varepsilon_{110}}{(\varepsilon_{tr}-\varepsilon_{110}+\varepsilon_{001}+\varepsilon_{tr}\varepsilon_{001})} \frac{A_{001}}{A_{110}}, \\
b &= \frac{(1+\varepsilon_{tr})(1+\varepsilon_{001})}{(\varepsilon_{tr}-\varepsilon_{110}+\varepsilon_{001}+\varepsilon_{tr}\varepsilon_{001})} \frac{A_{001}}{A_{110}}, \\
c &= \frac{(1+\varepsilon_{110})(\varepsilon_{tr}+\varepsilon_{001}+\varepsilon_{tr}\varepsilon_{001})}{(\varepsilon_{tr}-\varepsilon_{110}+\varepsilon_{001}+\varepsilon_{tr}\varepsilon_{001})}, \quad \text{and} \\
d &= -\frac{(1+\varepsilon_{110})}{(\varepsilon_{tr}-\varepsilon_{110}+\varepsilon_{001}+\varepsilon_{tr}\varepsilon_{001})}.
\end{aligned}\right\}
\tag{23}
$$

After the stresses in the phases [equation (9)] are determined from the constrained energy minimization, the elastic stress component σ_e in the wire can be obtained as

$$
\begin{aligned}
\sigma_e &= \frac{1}{V_0} \frac{\partial U}{\partial \varepsilon} = \frac{1}{V_0} \frac{\partial}{\partial \varepsilon} (V_{110}u_{110} + V_{001}u_{001} + Nu_{int}) \\
&= \frac{1}{V_0} \left(V_{110} \frac{du_{110}}{d\varepsilon_{110}} \frac{\partial \varepsilon_{110}}{\partial \varepsilon} + V_{001} \frac{du_{001}}{d\varepsilon_{001}} \frac{\partial \varepsilon_{001}}{\partial \varepsilon} \right) \\
&= \left(\frac{V_{110}}{V_0} \frac{\partial \varepsilon_{110}}{\partial \varepsilon} \right) \sigma_{110} + \left(\frac{V_{001}}{V_0} \frac{\partial \varepsilon_{001}}{\partial \varepsilon} \right) \sigma_{001}.
\end{aligned}
\tag{24}
$$

This stress component describes the thermodynamically reversible part of the deformation process. Note that equation (24) is also applicable to the wire as it deforms fully elastically in the $\langle 110 \rangle/\{111\}$ configuration before the initiation of the transformation ($V_{001}/V_0 = 0$ and $\varepsilon = \varepsilon_{110}$) and in the $\langle 001 \rangle/\{100\}$ configuration after the completion of the transformation ($V_{110}/V_0 = 0$ and $\varepsilon = \varepsilon_{001}$). For example, for the loading and unloading of a single $\langle 110 \rangle/\{111\}$ phase, $V_{110}/V_0 = 1$ and $\partial \varepsilon_{110}/\partial \varepsilon = 1$. Consequently, the stress reduces to that in the $\langle 110 \rangle/\{111\}$ phase, i.e., $\sigma = \sigma_{110}$. Similarly, for the loading and unloading of a single $\langle 001 \rangle/\{100\}$ phase, $V_{001}/V_0 = 1$ and $\partial \varepsilon_{001}/\partial \varepsilon = 1/(1 + \varepsilon_{tr})$, and $\sigma = \sigma_{001}/(1 + \varepsilon_{tr})$.

In order to calculate $\partial \varepsilon_{110}/\partial \varepsilon$ and $\partial \varepsilon_{001}/\partial \varepsilon$ for the lattice reorientation (loading) process, we consider an infinitesimal strain increment $d\varepsilon$ in the wire. This total deformation increment consists of contributions from the two phases [equations (13)–(15)], i.e.,

$$
l_0 \, d\varepsilon = l_{110}^0 \, d\varepsilon_{110} + l_{001}^0 \, d\varepsilon_{001}.
\tag{25}
$$

Also, the force balance condition in equation (18) can be rewritten as

$$
\frac{d\sigma_{110}}{d\varepsilon_{110}} \, d\varepsilon_{110} A_{110} = \frac{d\sigma_{001}}{d\varepsilon_{001}} \, d\varepsilon_{001} A_{001}.
\tag{26}
$$

Equations (24), (25), and (26) combine to give

$$
\sigma_e = \lambda_{110}\sigma_{110} + \lambda_{001}\sigma_{001},
\tag{27}
$$

where

$$
\left.\begin{aligned}
\lambda_{110} &= \frac{l_{110}^0}{l_{110}^0 + \left(\frac{A_{110}}{A_{001}}\right)\left(\frac{d\sigma_{110}}{d\varepsilon_{110}} \big/ \frac{d\sigma_{001}}{d\varepsilon_{001}}\right)l_{001}^0} \quad \text{and} \\
\lambda_{001} &= \frac{l_{001}^0}{\left(\frac{d\sigma_{001}}{d\varepsilon_{001}} \big/ \frac{d\sigma_{110}}{d\varepsilon_{110}}\right)l_{110}^0 + \left(\frac{A_{110}}{A_{100}}\right)l_{001}^0}.
\end{aligned}\right\}
\tag{28}
$$

Equation (28) specifies that, for any strain

$$\lambda_{110} + \lambda_{001}\frac{A_{110}}{A_{001}} = 1. \tag{29}$$

The implication of this relation is that σ_e is constant for the lattice reorientation (loading) process. This finding is consistent with the fact that the total force is constant in the analysis. The fact that σ_e is constant during the phase transformation can also be verified using strain energy which varies linearly for the lattice reorientation (loading) process. This fact significantly simplifies the constrained strain energy minimization calculation in that only the minimization at one strain during the phase transformation is required.

In the unloading process, reverse lattice reorientation takes place by the propagation of existing twin boundaries and, more importantly, by the nucleation and annihilation of twin boundaries at the critical strains, causing precipitous changes in the length fractions of the phases and resulting in rapid changes or discontinuities in stress. MD results show that the reverse lattice reorientation is accomplished primarily by the nucleation and annihilation of twin boundaries and these events define the critical strains [1–3], the propagation of the twin boundaries plays only a secondary role. Because of this, the length fractions of the phases do not change significantly from that at $\varepsilon = \varepsilon_{n-1}^c$ during the strain segment of $\varepsilon_{n-1}^c > \varepsilon > \varepsilon_n^c$ and the overall response of the nanowire is largely dominated by the elastic deformation of the phases. At the end of each segment $\left(\varepsilon = \varepsilon_n^c\right)$, another nucleation or annihilation event occurs and the length fractions of the phases change precipitously, leading to a new phase equilibrium state. The stresses and length fractions of the phases at the phase equilibrium states and throughout of period of $\varepsilon_{n-1}^c > \varepsilon > \varepsilon_n^c$ can be obtained via constrained energy minimization embodied in equations (11)–(19).

Dissipative Process

The thermodynamically irreversible part of the transformation process involves the initial nucleation and propagation of a twin boundary during loading, and the nucleation, propagation and annihilation of twin boundaries during unloading. The evolution of the total number of twin boundaries N for the 1.8×1.8 nm Cu wire during unloading from a strain of $\varepsilon = 0.34$ at four different temperatures between 150 and 450 K is shown in Fig. 3. The fully transformed $\langle 001 \rangle/\{100\}$ wire does not contain any twin boundary and undergoes elastic recovery at the beginning of the unloading process. The number of twin boundaries increases as unloading progresses and reaches a maximum approximately half way through the process. The number subsequently decreases and approaches zero when the wire
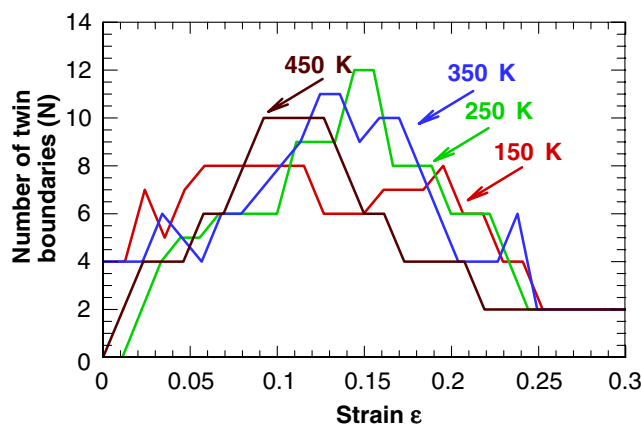
Fig. 3 The total number of twin boundaries as a function of strain during unloading of a 1.8×1.8 nm Cu wire

returns to the $\langle 110 \rangle/\{111\}$ state and its original length before the load cycle.

During loading, the single twin boundary propagates along the wire axis through sequential nucleation, glide and annihilation of partial dislocations [12, 13]. During unloading, multiple twin boundaries nucleate, annihilate and propagate. In this study, the interest is not in the mobility of individual twin boundaries or the local environments (e.g., local stress and available free energy) for individual twin boundaries. Rather, the interest is in capturing and quantifying the aggregate effect of the twin boundaries on the behavior of the nanowire. In an average sense, the dissipation stress associated with propagation of twin boundaries is assumed to be proportional to the total number of twin boundaries (N), i.e.,

$$\sigma_{\text{dissip}} = Nq_{\text{p}} \tag{30}$$

Here, q_{p} is the average contribution to the engineering stress σ by the propagation of one twin boundary for each unit increase in ε.

Equations (8), (10) and (30) combine to yield the stress–strain relation in terms of the Cauchy stress $\tilde{\sigma}$ as

$$\tilde{\sigma} = \begin{cases} (\sigma_e + q_p)(1+\varepsilon), & \text{loading;} \\ (\sigma_e - Nq_p)(1+\varepsilon), & \text{unloading.} \end{cases} \tag{31}$$

Comparison with Results of MD Simulations

The continuum model derived above is fitted to the results of a series of MD simulations of isothermal, macroscopically equilibrium tensile deformation of Cu nanowires. The hyperelastic responses of the pure $\langle 110 \rangle/\{111\}$ and $\langle 001 \rangle/\{100\}$ phases are required input for the continuum model. These functions are obtained from separate MD calculations for each wire size and temperature [8, 9]. The

critical strains $\left(\varepsilon_i^c\right)$, the critical stresses associated with them, and the total number of twin boundaries in the wire (N) are also determined from MD simulations. The elastic part of the stresses in the phases (σ_{110} and σ_{001}) associated with the equilibrium phase transition and the strains (ε_{110} and ε_{001}) of the two phases are determined through the constrained strain energy minimization. These elastic stress components allow σ_e in the wire to be obtained. The dissipative part of the total stress associated with propagation of one twin boundary (q_p) is obtained by fitting the model to the results of MD simulations.

The elastic responses of the phases are only weakly dependent on temperature over the temperature range of 150–450 K and, therefore, are not the source for the significant temperature dependence of wire behavior seen in the MD simulations. The effect of temperature on behavior comes primarily through the nucleation, propagation and annihilation of twin boundaries and is quantified by σ_{dissip}. Specifically, σ_{dissip} is lower at higher temperatures because thermal fluctuations facilitate overcoming the energy barrier for nucleation and annihilation of partial dislocations. For the same reason, the yield strain and the associated yield stress are also lower at higher temperatures. The behavior of a $\langle 110 \rangle / \{111\}$ Cu nanowire with the lateral size of 1.8×1.8 nm over 150–450 K is shown in Fig. 4. Obviously, very good agreement is obtained between the model and the MD data over the range of temperature analyzed. In the lattice reorientation during loading, the nominal stress is constant and the slow increase in the

Cauchy stress (Fig. 4) is due to the decrease in the average cross-sectional area with the strain. This characteristic of the nominal stress can also be found in phase transformations of other shape memory materials such as single-crystalline CuAlNi [14] and nano-grained NiTi [15]. Detailed analyses show that the contribution of the propagation of one twin boundary to the dissipative part of the stress (q_p) during loading is larger than that during unloading. This difference reflects the fact that the reverse lattice reorientation is primarily through the nucleation and annihilation of twinned boundaries and the forward lattice orientation occurs solely through the propagation of a twin boundary from the $\langle 001 \rangle / \{100\}$ region into the $\langle 110 \rangle / `\{111\}$ region. Fundamentally, the activation of propagation or nucleation/annihilation has to do with the relative magnitudes of the energy barriers associated with these processes. Obviously, the relative magnitudes are different for loading and unloading, giving rise to the different behaviors observed here. The quantification of these energy barriers is challenging and beyond the scope of the current paper.

Concluding Remarks

A continuum model is developed to characterize the tensile loading and unloading behavior of shape memory metal nanowires. This model decomposes the lattice reorientation and the reverse lattice reorientation processes into reversible smooth transitions between metastable phase-equilibrium

Fig. 4 Comparison of MD results with the prediction of equation (31) for a 1.8×1.8 nm Cu wire at (**a**) 150, (**b**) 250, (**c**) 350, and (**d**) 450 K
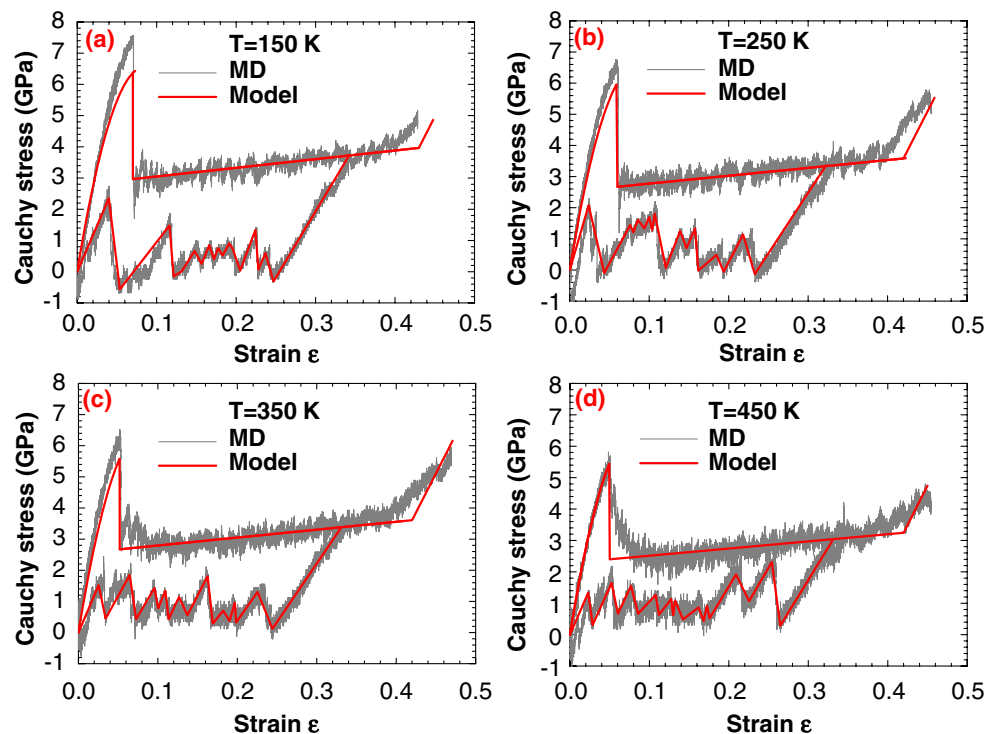
states and irreversible dissipative twin boundary nucleation, propagation and annihilation events. During the lattice reorientation in loading, the length fractions of the phases vary smoothly. During the reverse lattice reorientation in unloading, discontinuities arise due to the nucleation and annihilation of twin boundaries. The energy dissipation associated with the nucleation, propagation and annihilation of twin boundaries is the primary mechanism responsible for the hysteresis stress–strain loop and the underlying pseudoelasticity. It is worthwhile to point out that similar pseudoelastic behaviors can be induced by other phase transformations, such as the one in ZnO nanowires reported and characterized in [16, 17].

References

1. Liang W, Zhou M (2005) Pseudoelasticity of single crystalline Cu nanowires through reversible lattice reorientations. J Eng Mater Technol 127(4):423–433. doi:10.1115/1.1928915.
2. Liang W, Zhou M (2006) Atomistic simulations reveal shape memory of fcc metal nanowires. Phys Rev B Condens Matter Mater Phys 73:115409. doi:10.1103/PhysRevB.73.115409.
3. Liang W, Zhou M, Ke F (2005) Shape memory effect in Cu nanowires. Nano Lett 5(10):2039–2043. doi:10.1021/nl0515910.
4. Park H, Gall K, Zimmerman JA (2005) Shape memory and pseudoelasticity in metal nanowires. Phys Rev Lett 95:255504. doi:10.1103/PhysRevLett.95.255504.
5. Park H, Ji C (2006) On the thermomechanical deformation of silver shape memory nanowires. Acta Mater. 54:2645–2654. doi:10.1016/j.actamat.2006.02.006.
6. Ji C, Park HS (2007) The effect of defects on the mechanical behavior of silver shape memory nanowires. J Comput Theor Nanosci 4:1–10. doi:10.1166/jctn.2007.025.
7. Park H, Gall K, Zimmerman J (2006) Deformation of FCC nanowires by twinning and slip. J Mech Phys Solids 54:1862–1881. doi:10.1016/j.jmps.2006.03.006.
8. Liang W, Srolovitz DJ, Zhou M (2007) A micromechanical continuum model for the tensile behavior of shape memory metal nanowires. J Mech Phys Solids 55:1729–1761. doi:10.1016/j.jmps.2007.01.001.
9. Liang W, Zhou M (2007) Discovery, characterization and modelling of novel shape memory behaviour of fcc metal nanowires. Philos Mag A 87:2191–2220. doi:10.1080/14786430701280943.
10. Liang W, Zhou M (2004) Response of copper nanowires in dynamic tensile deformation. J Mech Eng Sci 218(6):599–606. doi:10.1243/0954405041167158.
11. Vainchtein A, Rosakis P (1999) Hysteresis and stick–slip motion of phase boundaries in dynamic models of phase transitions. J Nonlinear Sci 9:697–719. doi:10.1007/s003329900083.
12. Abeyaratne R, Knowles JK (1993) A continuum model of a thermoelastic solid capable of understanding phase transitions. J Mech Phys Solids 41:541–571. doi:10.1016/0022-5096(93)90048-K.
13. Abeyaratne R, Vedantam S (2003) A lattice-based model of the kinetics of twin boundary motion. J Mech Phys Solids 51:1675–1700. doi:10.1016/S0022-5096(03)00069-3.
14. Zhang X, Sun Q, Yu S (2000) A non-invariant plane model for the interface in CuAlNi single crystal shape memory alloys. J Mech Phys Solids 48:2163–2182. doi:10.1016/S0022-5096(99)00102-7.
15. Sun Q, Li Z (2002) Phase transformation in superelastic NiTi polycrystalline micro-tubes under tension and torsion—from localization to homogeneous deformation. Int J Solids Struct 39:3797–3809. doi:10.1016/S0020-7683(02)00182-8.
16. Kulkarni A et al (2006) Novel phase transformation in ZnO nanowires under tensile loading. Phys Rev Lett 97:105502. doi:10.1103/PhysRevLett.97.105502.
17. Kulkarni A, Zhou M (2008) Continuum characterization of novel pseudoelasticity of ZnO nanowires. J Mech Phys Solids 56:2473–2493. doi:10.1016/j.jmps.2008.02.005.
18. Plimpton SJ (1995) Fast parallel algorithms for short-range molecular dynamics. J Comput Phys 117:1–19. doi:10.1006/jcph.1995.1039.